Title
KINETIC ENERGY RELEASE IN HEAVY- ION-INDUCED FISSION REACTIONS

Authors
Viola, Victor E.
Sikkeland, Torbjorn.

Publication Date
1962-10-31

UCRL-10284

University of California

Ernest O. Lawrence Radiation Laboratory

KINETIC ENERGY RELEASE IN HEAVY-ION-INDUCED FISSION REACTIONS

Berkeley, California

DISCLAIMER

UCRL-10284 -
correct figs added
4-23-63

UNIVERSITY OF CALIFORNIA

Lawrence Radiation Laboratory

Berkeley, California

Contract No. W-7405-eng-48

KINETIC ENERGY RELEASE IN HEAVY-ION-INDUCED FISSION REACTIONS

Victor E. Viola, Jr. and Torbjørn Sikkeland

October 31, 1962

UCRL-10284

KINETIC ENERGY RELEASE IN HEAVY-ION-INDUCED FISSION REACTIONS

Victor E. Viola, Jr. and Torbjørn Sikkeland

Lawrence Radiation Laboratory
University of California
Berkeley, California

October 31, 1962

ABSTRACT

The most probable kinetic energy release in fission reactions induced by 125-MeV C^{12} ions and 166-MeV O^{16} ions has been measured for the target nuclei Pr^{141}, Tb^{159}, Ho^{165}, Tm^{169}, Lu^{175}, Au^{197}, Bi^{209}, Th^{232}, U^{238}, and Pu^{240}. Silicon diode surface-barrier detectors were used in these measurements, and a Cf^{252} spontaneous-fission source served as the absolute energy standard. A least-squares analysis of our data and that obtained by others gives $\bar{E}_K(\text{MeV}) = 0.1065\ Z^2/A^{1/3} + 20.1$. The dependence of the most probable kinetic energy on the scission shape of the fissioning nucleus has been examined by comparison with recent calculations based on the work of Cohen and Swiatecki. The data are consistent with scission shapes corresponding to spheroids whose shapes minimize the total energy of the system.

The most probable kinetic energy release has been found to be essentially independent of the excitation energy of the compound nucleus. It is also observed that the full width at half-maximum of the kinetic energy distribution is relatively constant for values of the fissionability parameter x less than 0.7, but increases rapidly above this value. The half-width also exhibits an increased spread as the excitation energy of the compound nucleus increases.

KINETIC ENERGY RELEASE IN HEAVY-ION-INDUCED FISSION REACTIONS

Victor E. Viola, Jr. and Torbjørn Sikkeland

Lawrence Radiation Laboratory
University of California
Berkeley, California

October 31, 1962

I. INTRODUCTION

The fragment kinetic energy release is one of the few fundamental properties of nuclear fission for which one can give the experimental results a rather quantitative theoretical interpretation in terms of the liquid-drop model.[1,2] Until recently, however, liquid-drop calculations which could be compared with kinetic energy release data were not available. Consequently, such comparisons were restricted to only the simplest of models.

Terrell has correlated the most probable kinetic energy release in fission, $\bar{E}_K$, with $Z^2/A^{1/3}$ of the fissioning nucleus.[3] This parameter is proportional to the Coulomb energy between two uniformly charged liquid drops. Over a limited range of values, Terrell is able to fit the data quite well with the function $\bar{E}_K = 0.121Z^2/A^{1/3}$ MeV. Assuming the fissioning nucleus to be represented by two spheres in contact, Terrell obtained a value of $r_o = 1.82$ F for the nuclear radius parameter. This large value of r_o has been ascribed to deformation of the fragments from a spherical shape at the scission point and to a tendency of the protons of the two separating nuclei to be more separated than the neutrons. He also suggests that this result may be due to expansion of the highly excited fragments, contrary to the generally accepted assumption that the nuclear density remains constant.

The Coulomb interaction energy is quite sensitive to the separation distance of the fragment charge centers. This distance depends upon the shape of the nucleus at scission. Any model that proposes to explain fission-fragment kinetic-energy-release data must therefore consider the shape of the fissioning nucleus as it deforms toward scission. The liquid-drop-model calculations of Swiatecki, and Cohen and Swiatecki,[4-7] indicate that there is a distinct variation in the elongation of saddle-point shapes as a function of the fissionability parameter x [where $x = (Z^2/A)/(Z^2/A)_{crit}$ and $(Z^2/A)_{crit} = 50.13$]. This variation should be reflected in the configuration of the nucleus at scission. Hence, simple shapes other than spheres, e.g., spheroids whose eccentricity depends on x, should furnish a model of the nucleus at the scission point that is more consistent with existing theory. Cohen and Swiatecki[7] have considered this in their recent calculations, which are discussed Sec. III A.

Experimentally, the study of fission reactions can be extended to much lower x values than previously attainable. Bombardment with heavy ions provides sufficient excitation energy to overcome the fission barriers for target nuclei in the rare-earth region.[8,9] By measuring the fission kinetic-energy release in this region, a more thorough examination of the dependence of $\bar{E}_K$ on the scission shape can be obtained.

Heavy-ion-induced fission studies can also be used to determine whether or not any of the excitation energy of the compound nucleus is transformed into kinetic energy of the fragments. This can be accomplished either by variation of the bombarding energy or by forming a compound nucleus at high excitation energy for which $\bar{E}_K$ is known from low-energy fission.

Cohen and Swiatecki have also suggested that for values of the

fissionability parameter x near 0.7, the sequence of equilibrium saddle-point shapes undergoes a rapid change from the Frankel-Metropolis family to the Bohr-Wheeler family as x increases.[10] This implies that across this transition region one might expect to observe a spreading out of the mass and kinetic energy distributions of the fragments.

The object of our research was to examine the dependence of the average kinetic energy release in fission on $Z^2/A^{1/3}$ and x for a large number of fissioning species spanning the region x = 0.7. In addition it was desired to investigate further the dependence of $\overline{E}_K$ on excitation energy. Analysis of these spectra then permits one to learn the nature of the distribution of masses and/or kinetic energies of the fissioning nuclei as a function of x.

II. EXPERIMENTAL PROCEDURE

The experimental arrangement has been described in a previous paper.[8] Heavy-ion beams were obtained from the Berkeley HILAC, which accelerates particles to 10.4 MeV/nucleon. The beam was magnetically analyzed and deflected 30 deg before reaching the fission chamber.

The target, located in the center of the chamber, could be oriented at various angles to the beam. Targets of $_{59}Pr^{141}$, $_{65}Tb^{159}$, $_{67}Ho^{165}$, $_{69}Tm^{169}$, $_{71}Lu^{175}$, $_{79}Au^{197}$, $_{83}Bi^{209}$, $_{90}Th^{232}$, $_{92}U^{238}$, and $_{94}Pu^{240}$ were made by vaporizing the material onto a 110-$\mu g/cm^2$ nickel foil. Target thicknesses ranged from about 100 to 300 $\mu g/cm^2$, except for Th^{232}, which was approximately 600 $\mu g/cm^2$.

The fission fragments were detected by a silicon-diode crystal of resistivity 15 Ω-cm and covered with 50 $\mu g/cm^2$ gold.[11] The bias on the semiconductor was 6 V. The angular position of the detector θ_{lab}, relative to the beam, could be adjusted to within 1/4 deg. This was achieved by counting elastically scattered beam particles on each side of the beam axis.

The electronic system was, except for a few modifications, the same as in reference 8. After proper amplification the pulses were analyzed by a Penco 100-channel pulse-height analyzer. A pulse from a pulse generator was used to check the gain stability and resolution of the system. A signal from the HILAC electronic system triggered the pulse generator so that any gain shift during the 2-msec beam burst could be recorded. The gain shift was a function of the number of particles entering the detector and thus depended on the beam level and the detector angle θ_{lab}. We adjusted the beam level to keep the gain shift to 0.5 channel or less, corresponding to less than 3/4 MeV, and the data were corrected accordingly. The resolution

was around 1%. With the wide distribution in kinetic energy observed in fission, this implied that no correction in the observed widths had to be applied.

A. Kinetic Energy Determination

The pulse-height spectrum of the fragments in heavy-ion-induced fission shows a symmetric distribution around a most probable pulse height, as shown in Fig. 1. The average pulse height is therefore equal to the most probable pulse height.

The quantity of interest is $E_{c.m.}^{i}$, the most probable fragment kinetic energy in the center-of-mass (c.m.) system of the fissioning nucleus before the prompt-neutron emission from the fragments. Evaporation of neutrons from the fragments does not change the average velocity, but it does lower the c.m. kinetic energy to some final value $E_{c.m.}^{f}$. The conversion of $E_{c.m.}^{f}$ to $E_{c.m.}^{i}$ is discussed in Sec. II C. The energy $E_{c.m}^{f}$ corresponds to an energy in the laboratory (lab) system E_{lab} related to $E_{c.m.}^{f}$ according to the equations:

$$E_{lab} = E_{c.m.}^{f} (1 + X^2 + 2X \cos \theta_c), \qquad (1)$$

$$\tan \theta_{lab} = \sin \theta_c / (X + \cos \theta_c), \qquad (2)$$

$$X = v_{fn}/v_{ff}, \qquad (3)$$

where v_{fn} is the velocity component of the fissioning nucleus along the beam

axis; v_{ff}, the most probable velocity of the fragments; and θ_c, the fragment angle with respect to the beam axis in the c.m. system. The quantity X^2 is determined directly in fission-fission angular-correlation experiments.[8,12] Then $E_{c.m.}^{f}$ can be found by measuring E_{lab} at one angle.

The fragments having an energy E_{lab} suffer energy losses in the target ΔE_t and in the "window" of the crystal ΔE_w. This window consists of the gold and an oxide layer on the surface of the detector. In addition, we might expect an energy defect ΔE_D in the crystal, resulting from either incomplete collection of the ions formed or from an ionization defect. We then have:

$$E_{lab} = \Delta E_t + \Delta E_w + \Delta E_D + E_{cr}. \qquad (4)$$

Here E_{cr} is the energy properly recorded by the crystal. Presumably the pulse height should be linear with E_{cr} and independent of the mass of the fragment. The other quantities may be functions of both mass and energy of the particle.

The correction ΔE_t is found by observing the pulse-height shift, as a function of the angle of the target. By varying the thickness of the target seen by the fragments moving towards the detector, an extrapolation to zero thickness can be achieved.

Similarly, ΔE_w may be found by tilting the detector relative to the incoming fragments. One cannot, however, obtain a quantitative number for ΔE_w at the same time because the path of the fragments changes in direction relative to the electric field in the detector. A change towards

higher collection efficiency can then take place. Instead, the pulse height vs the quantity ($\Delta E_w + \Delta E_D + E_{cr}$) for individual masses can be determined directly by a method first used by Sikkeland and briefly described in reference 8. This method will be described in some detail in the following section.

B. Energy Calibration

The energy ($\Delta E_w + \Delta E_D + E_{cr}$) vs pulse height for mass 106 fragments was first determined. This mass was chosen because it corresponds to the light-fragment peak in the Cf^{252} spontaneous fission (SF) spectrum and the most probable mass in fission from $Bi^{209} + O^{16}$ bombardments. The light fragments from a weightless Cf^{252} source ($\Delta E_t = 0$) have an energy of 103 MeV (after neutron emission from the fragments).[13] The energy of the fragments from the $Bi^{209} + O^{16}$ system varies with θ_{lab} according to Eq. (1).

The most probable pulse height vs θ_{lab} for the system $Bi^{209} + O^{16}$ was then determined. After correcting for ΔE_t, the most probable pulse height was found to be equal to the pulse height of the Cf^{252} SF light peak at $\theta_{lab} = 51$ deg. Because the masses and pulse heights are equal, the kinetic energy of the fragments from the two sources must be the same, namely 103 MeV. With an X^2 value[8] of 0.066 we find $E_{c.m.}^{f}$ to be 78.6 MeV. The variation of E_{lab}, and thus with the pulse height, is then calculated from Eq. (1). The resulting ($\Delta E_w + \Delta E_D + E_{cr}$) vs pulse-height curve for mass 106 is shown in Fig. 2. We see that for the energies with which we are dealing the curve is a straight line, the extrapolation of which intercepts the electrical zero. We would like to comment on this result.

As was stated above, E_{cr} vs pulse height should give a straight line

through the electrical zero at $E_{cr} = 0$. The variation of ΔE_w with energy is known from range-energy studies of fission fragments.[14] The dE/dX decreases with decreasing fragment energy and approaches zero except just before the end of the fragment range (at very low energy) where dE/dX becomes very large. Qualitatively, this means that the ΔE_w will decrease with decreasing energy. Similarly, ΔE_D is expected to decrease with energy because the ion density—and consequently, the chance for recombination,—decreases with decreasing energy. Therefore E_{lab} approaches E_{cr} as the energy is decreased, and appears to go through the electrical zero at $E_{lab} = 0$. We should, however, expect the curve to deviate from a straight line at very low energies.

The E_{lab} vs pulse-height calibration curve for other masses was constructed as follows. First, we assumed a linear variation of $(\Delta E_w + \Delta E_D + E_{cr})$ vs pulse height, and an intercept at the electrical zero. The Cf^{252} SF heavy-fragment peak gives the energy vs pulse height for the mass 144, which has an energy of 79 MeV.[13] Similarly, one can use the pulse height of the valley in the Cf^{252} SF spectrum corresponding to a mass of about 124 and energy 90.3 MeV.[13] These points are given in Fig. 2. We observe that at the same energy the heavier mass gives a smaller pulse height. This is partly explained by the larger ΔE_w for the heavier fragment at these energies. Also ΔE_D is expected to increase with increasing mass A_f of the fragment, since the ionization density increases and with that, the chance for recombination. Another way of stating these results is that at a certain pulse height, the corresponding E_{lab} increases with A_{lab}. At a pulse height that is equivalent to $E_{lab} = 79$ MeV for $A_f = 144$, we find, typically, $E_{lab} = 75$ MeV for $A_f = 106$, or $(\Delta E_w + \Delta E_D)/A_f \approx 0.1$ MeV/nucleon.

Our second assumption then is that this mass relation holds in the mass range 80 to 120 amu; thus an E_{lab} vs pulse-height curve for the fragments investigated here can be constructed.

A satisfactory check on the consistency of these assumptions was achieved by measuring E_{lab} at two widely different angles and comparing the values for $E_{c.m.}^{f}$. They were found to be the same, well within the limits of error.

This dependence of the pulse height upon the mass of the fragments introduces corrections in E_{lab} relative to the energy-pulse-height curve for mass 106 of the order of, at most, 2 MeV. We assume the uncertainty in these corrections to be 50%, which we consider a safe estimate. Other errors involved in the measured E_{lab} are due to errors in ΔE_t, which we assume are ±30%, and uncertainty in estimation of the most probable peak of 0.5 channel, corresponding to about 0.5 to 0.8 MeV. In the estimation of $E_{c.m.}^{f}$, errors are introduced due to uncertainty in X^2. These errors are quite low, and when the measurements are performed at $\theta_{lab} = 90$ deg, they are negligible. We have also considered the contribution to the kinetic energy distribution of direct-interaction fission reactions in which a compound nucleus is not formed.[8]

Table I lists the systems with the corresponding $E_{c.m.}^{f}$ values.

C. Prompt-Neutron Emission

To compare these data with measured values of the kinetic energy release in spontaneous fission and in fission induced by lighter projectiles, it is desireable to know the initial kinetic energy of the fragments before prompt-neutron emission, $E_{c.m.}^{i}$. Application of this correction requires a knowledge of both the average number of neutrons evaporated from the compound nucleus before fission and the number of prompt neutron, $\bar{\nu}$, emitted from the separating fragments. These corrected values for $\bar{E}_K$ will then describe the kinetic energy of the fragments immediately after scission.

Compilations by Huizenga and Vandenbosch[15] show that at these excitation energies one should expect essentially first-chance fission for nuclei with $x > 0.7$. The neutron-evaporation to fission-level-width ratios for lower x values are not well characterized for heavy-ion reaction. However, the high fission barriers for these nuclei —combined with the large excitation energies and angular momenta of compound systems formed in heavy-ion reactions—should make first-chance fission highly probable. The values for $E_{c.m.}^{i}$ used in the discussion section were calculated on this assumption.

Assuming the most probable fission event to be binary and symmetric, we determined $\bar{\nu}$ as follows: First, from the energy balance between the c.m. energy of the system, the Q value of the fission event, and the kinetic energy release in the reaction, the excitation energy of the fragments could be calculated. The Q values were estimated from the mass tables of Cameron.[16] As a first approximation for the kinetic energy release, we used the experimental value of $E_{c.m.}^{f}$. The number of neutrons that could be evaporated from these fragments was determined, assuming each neutron reduced the excitation energy of the parent fragment by an amount $B_n + 2T$. Here B_n is the binding

energy of the neutron, taken from Cameron.[16] The nuclear temperature T was approximated by the relationship $T = \sqrt{10E^*/A}$, where E^* is the excitation energy at each step in the evaporation chain. This gave a first approximation to $\bar{\nu}$ and $E_{c.m.}{}^{i}$. Successive values of $E_{c.m.}{}^{i}$ were obtained in this way until the kinetic energy converged on the final value. In each case the final excitation energy was presumed to be 4 to 6 MeV per fragment, to account for energy dissipated in gamma emission and that tied up in rotational energy of the fragments. The values of $\bar{\nu}$ and $E_{c.m.}{}^{i}$ are listed in Table I. The errors include an allowance for an error of one neutron in estimating $\bar{\nu}$.

As an opposite extreme, we have also estimated $E_{c.m.}{}^{i}$ values for $x < 0.7$, assuming that neutrons are evaporated from the compound nucleus until an excitation energy just above the fission barrier is reached. The fission barriers were estimated from the relationship derived by Huizenga et al.[17] The effect of this assumption is discussed in the following section.

We have recently measured the fission excitation functions for rare-earth targets bombarded by heavy ions.[18] The fission cross sections decrease quite rapidly with decreasing energy. That is, the slope of the excitation function becomes quite steep at energies well above both the Coulomb barrier and the fission thresholds from reference 17. These results give added weight to the former assumption that fission is occurring early in the deexcitation chain. In addition, it was presumed that charged-particle evaporation before fission does not affect the data substantially. These charged-particle evaporation cross sections are less than 10% of the reaction cross section for Au and Bi[19], although this result does not necessarily apply for targets of lower Z. This resulting value is an upper limit for fission events preceded by charged-particle evaporation.

III. DISCUSSION OF RESULTS

As mentioned previously, Terrell has shown that $\bar{E}_K$ varies linearly with $Z^2/A^{1/3}$ of the fissioning nucleus, over a limited region.[3] The parameter $Z^2/A^{1/3}$ is proportional to the electrostatic potential energy one would expect for two uniformly charged nuclei of mass A_1, A_2, represented by point charges Z_1e, Z_2e, and whose charge centers are spearated by a distance d at the scission point. If one assumes that distance $d = d_o(A_1^{1/3} + A_2^{1/3})$, where d_o is a constant, then we may write

$$\bar{E}_K = \frac{Z_1 Z_2 e^2}{d_o(A_1^{1/3} + A_2^{1/3})}. \qquad (4a)$$

For symmetric charge and mass division, this becomes

$$\bar{E}_K = \frac{Z^2 e^2}{2^{8/3} d_o A^{1/3}} = \text{constant} \times \frac{Z^2}{A^{1/3}}, \qquad (4b)$$

where Z and A refer to the fissioning nucleus. The relationships (4a) and (4b) predict nearly the same value of $\bar{E}_K$ for asymmetric charge and mass division. This difference amounts to but a few percent for Cf^{252}.

In Figs. 3 and 4 we have plotted the measured values of $\bar{E}_K$ before prompt-neutron emission vs $Z^2/A^{1/3}$ of the fissioning nucleus. Figure 3 contains the results from this work. Figure 4 includes most of the data

compiled earlier by Terrell,[3] plus recent data of Britt et al.,[20] and a new measurement of the Fm^{254} spontaneous-fission energy by Brandt.[21] The data of reference 20, which are in the region of $Z^2/A^{1/3} \approx 1200$, are in good agreement with those recently reported by Vandenbosch and Huizenga.[22] By using all of these data, a least-squares analysis revealed that $\bar{E}_K$ was not simply a linear function of $Z^2/A^{1/3}$ with zero intercept. The function $\bar{E}_K = 0.121\ Z^2/A^{1/3}$ was far outside the limits of error for $\bar{E}_K$ at the lower $Z^2/A^{1/3}$ values measured in this work.

By using a general linear least-squares function, an excellent fit to our data and those of references 3, 20, 21 and 22 was obtained with the relationship

$$\bar{E}_K \text{ (MeV)} , (0.1065\ Z^2/A^{1/3}) + 20.1 \qquad (5)$$

This function is drawn through the data in both Figs. 3 and 4.

The above relationship is based upon results that assume first-chance fission. If neutron evaporation precedes fission until just above the fission barrier[17] when $x < 0.7$, then one obtains

$$\bar{E}_K \text{ (MeV)}, (0.1144\ Z^2/A^{1/3}) + 7.9. \qquad (6)$$

Although this function gives somewhat better agreement with Terrell's relationship,[3] the assumption on which it is based seems rather extreme at the present time. For $x < 0.7$ it is known that the probability for fission

increases rapidly with increasing excitation energy and angular momentum.[9,17,18] Because these nuclei have large fission barriers, as well as high angular momenta and excitation energies, fission would be expected to occur early in the deexcitation chain, as previously stated.

A. Dependence of $\bar{E}_K$ on Scission Shape

Here we discuss the experimental results in terms of the liquid-drop model of fission.[1,2] Because of the complexity of the fission process, it is convenient to idealize the nucleus as a uniformly charged incompressible liquid drop. The competition between the attractive short-range nuclear force, approximated by a surface tension, and the repulsive long-range Coulomb force determines the shape of the drop. The threshold for fission occurs when the distortion of the drop becomes sufficiently large that the short-range nuclear force just balances the Coulomb force. The shape of the drop at this point is defined as the saddle point. Once the saddle-point shape is reached, further deformation leads irreversibly to scission of the drop. The scission shape is represented by two distinct drops at the moment of division.

The electrostatic interaction energy for separation to infinity of two charged drops is given by the dimensionless parameter

$$\xi = E_K/E_S^{(o)},$$

where $E_S^{(o)} = 17.81\ A^{2/3}$ MeV, the surface energy of the original undistorted drop.[23] The experimental values of ξ are given in Table I along with the fissionability parameter x for each system. In the following discussion

these values will be compared to calculated values for various scission-point configurations. In all the calculations, a value of r_o = 1.216 F, taken from Green's mass formula, is used for the nuclear radius parameter.[24] This value is consistent with the nuclear-charge distribution determined from electron-scattering results,[25] which should be of primary importance in considerations of the electrostatic interaction energy. We will assume binary fission with the two separating fragments of equal charge and mass, consistent with the fact that symmetric fission is the most probable event in heavy-ion-induced fission reactions.

1. Tangent Spheres

If one assumes the scission shape to be represented by tangent spheres, a value of d_o, or in this case r_o, equal to 2.12 F is obtained from the slope of Eq. (5). This value is to be compared with r_o = 1.82 F from Terrell's relationship[3] and about 1.2 F from Green's mass formula[24] and the electron-scattering data.[25] The tangent-sphere interaction energy ξ_I derived from an r_o of 1.216 F is shown with the experimental points in Fig. 5.

It seems most likely that the meaning of this discrepancy in r_o is that tangent spheres are a poor representation of the shape of the fission fragments at the scission point. Shapes more consistent with the liquid-drop theory are obtained if the two fragments are allowed to be spheroidal at the scission point. Thus the charge centers will be further removed than in the case of tangent spheres of the same total volume, lowering E_K. We cannot rule out the arguments[3] that this large value of r_o arises from (a) the protons being separated by a greater average distance than the neutrons at scission, or (b) a lower nuclear density due to the high excitation of the drop. However, in view of the following results, it appears that these are

secondary effects.

2. Colinear Spheroids

Recently Cohen and Swiatecki have, as an approximation to the more exact liquid-drop calculation, developed the formulae for calculating the surface and electrostatic energies of two uniformly charged colinear spheroids[7] The total energy of the system for varying ratios of the major to minor axes C/A is characterized by a specific minimum for a given value of the fissionability parameter x. Below x = 0.67 this minimum energy corresponds to the threshold for fission, and the optimum value of C/A so obtained[7,10] characterizes the saddle-point shape below x = 0.7.

In addition, Cohen and Swiatecki have performed computer calculations of the equilibrium liquid-drop saddle-point shapes and thresholds as a funtion of x.[26] These results were obtained by minimizing the energy of systems for shapes derived from expansion about a sphere in terms of Legendre polynomials of even order up to order 18. The previously mentioned transition in saddle-point shapes from the dumbbell-like Franekl-Metropolis family below $x \approx 0.7$ to the cylindrical Bohr-Wheeler family at larger x values[10] must be considered in comparisons of these two calculations. Below x = 0.7 the spheroid approximation to the saddle shapes and thresholds is in good agreement with the more exact calculations based on expansion about a sphere in terms of Legendre polynomials.[26] However, above this value of x, shapes predicted by the spheroid approximation deviate substantially from those of Legendre polynomial expansion. This simply means that as the saddle shape becomes more cylindrical, i.e., the necking-in becomes smaller, spheroids become a poorer representation of the saddle shape.

According to the definition of the saddle and scission points, the two-sphere model can appropriately be called a scission shape; i.e., it

represents a two-body configuration. The agreement vetween these thresholds and the exact saddle-point thresholds below x = 0.7 indicates that the saddle and scission points are nearly identical in this region. This agreement, as well as its disappearance at higher x, is readily associated with the necking-in of the saddle-point shape, which becomes important near x = 0.7. That is, the saddle shapes of the Frankel-Metropolis family are very nearly two-fragment configurations, while for the Bohr-Wheeler family, the shape must undergo considerable additional deformation before division occurs. Nonetheless, the two-spheroid model may still be an adequate description of the scission shapes above x = 0.7. The comparison of the electrostatic interaction energy predicted by these models with the experimental value of ξ thus makes it possible to gain some insight into the fragment configuration at the scission point.

Because the two-spheroid, or scission, thresholds for the Bohr-Wheeler family are lower than those of the exact-liquid-drop calculation, it is possible that some kinetic energy may be accumulated by the fragments in descending from the saddle point to the scission point. This then would result in an additional amount of energy to be added to the calculated value for the electrostatic interaction energy. We shall call this $\Delta\xi$, the difference in total energy between the saddle shapes calculated from the Legendre polynomial expansion[26] and the scission shapes of the two-spheroid model.

Halpern has argued that very little of this energy differnce, $\Delta\xi$ goes into kinetic energy of the fragments.[27] This conclusion is based upon the average number of evaporated neutrons per fission observed in the spontaneous fission of Pu^{240} and in neutron-induced fission of Pu^{239}. For the latter case $\bar{\nu}$ is greater than that for spontaneous fission by an amount

that can be readily accounted for by the differences in excitation energies for these systems. The implication here is that there must be thermal equilibrium on descent from the saddle point, at least up to the point where a spontaneously fissioning nucleus emerges from the barrier. Thus, the energy difference $\Delta\xi$ would be expected to appear as excitation energy of the fragments rather than in the form of kinetic energy. However, because the role of this energy difference is uncertain, it has been added as a dashed line to all the theoretical ξ values. Calculation of $\Delta\xi$ is based on results of Cohen and Swiatecki.[26]

a. Tangent spheroids. In Fig. 5 the experimental ξ values are also compared with the interaction energy calculated from a tangent-spheroid configuration. In addition to translational motion of separation, the actual fission fragments can be expected to undergo vibrational motion as they separate.

If the period of vibration is slow with respect to the velocity of separation, the interaction energy can be well approximated by permitting the two spheroids to retain their scission-point eccentricity along the entire axis of separation. This assumption is represented by the curve ξ_{II} in Fig. 5. The calculated curve falls somewhat above the experimental points. However, this model, as well as those described in the succeeding paragraphs, agrees with the data much better than that of tangent spheres.

On the other hand, if, after the fissioning nucleus snaps, the vibrational period of the fragments is rapid with respect to separation, the two fragments may oscillate back and forth between the initial prolate spheroid and an oblate spheroid. A simple approximation to this case is

given by the interaction energy for two spheres having the same volume and distance between charge centers as the initial spheroids. However, a more realistic comparison is provided by the recent calculations of Nix.[28] He has calculated the interaction energy for two liquid drops, having the scission-point deformations determined by Swiatecki, by solving the classical equations of motion for the drops as they separate to infinity. These results are given as ξ_{III} in Fig. 5 and are very nearly the same as the case for the approximation using two separated spheres.

Figure 6 presents the equilibrium saddle shape for $x = 0.60$ calculated from the liquid-drop expansion in terms of Legendre polynomials, with the scission shape corresponding to the tangent spheroids giving the electrostatic energies ξ_{II} and ξ_{III}. Because the saddle and scission shapes are expected to be nearly the same for this x value, the observed agreement is encouraging. However, the tangent-spheroid model predicts fission thresholds that are slightly higher than the exact liquid-drop calculations[7,26] for $x < 0.7$. This indicates that one may be able to find a somewhat better approximation to the saddle shapes.

b. Separated spheroids. In order to reproduce the liquid-drop thresholds more exactly, Milton and Wilber[29] have used the Cohen and Swiatecki[26] results to predict the properties for two colinear spheroids whose tips are separated by a distance characterized by a parameter D, given by

$$\frac{\text{separation distance}}{R_o} = \left(\frac{4\pi}{3}\right)^{1/3} D ,$$

where R_o is equal to $r_o A^{1/3} F$. The equilibrium configurations of the spheroids were calculated as described previously. By using D = 0.2, it was found that the equilibrium saddle-point thresholds for $x < 0.7$ could be reproduced quite well. Furthermore, this value of D gives agreement with the average excitation of Cf^{252} fragments deduced from their neutron-emission properties, assuming that this energy is represented by the distortion energy of the spheroids at scission.[30]

In Fig. 7 the data are compared with the interaction energy ξ_{IV} for spheroids with D = 0.2, assuming vibration to be slow with respect to separation. Also shown is the interaction energy ξ_V obtained from Nix's calculation for this case, which permits the spheroids to oscillate in shape as they separate.[28] For $x > 0.70$ the possible increase in energy gained in rolling downhill from the saddle point to the scission point is again indicated as a dashed line. Figure 8 gives the comparison between the scission shapes for ξ_{IV} and ξ_V and the liquid-drop shape for x = 0.60.

Figures 5 to 8 show that the $\bar{E}_K$ data can be described remarkably well by using the Cohen-Swiatecki model for scission shapes. Particularly good agreement is achieved with either of two models:

(a) Case III - two colinear spheroids that are allowed to oscillate between prolate and oblate shapes as they separate—assuming that any energy difference between the saddle and scission points appears as kinetic energy of the fragments; and

(b) Cases IV and V - two colinear spheroids with D = 0.2—assuming only Coulomb interaction contributes to the kinetic energy.

Depending upon the influence of the neck at scission, the actual scission shapes probably lie somewhere between the tangent spheroid and the

D = 0.2 separated spheroid models. Without a knowledge of the effects of distortion energy and the perturbations introduced by the approximation to the shapes, as well as smaller limits of error on the data, it is not worthwhile to attempt to discern the scission shapes more accurately. However, the qualitative results of these comparisons illustrate that the large value of r_o obtained from the tangent-sphere model most likely originates in the fact that this configuration is not a good representation of the actual case. The success obtained with the simple models discussed above shows that the fragment shapes can account for the observed kinetic-energy-release data quite well. Hence, it seems unnecessary to invoke more subtle effects, such as an expanded nuclear density, to explain $\bar{E}_K$ data.

B. Dependence of $\bar{E}_K$ on Excitation Energy

In the study of fission from compound nuclei of high excitation energy, it is also of interest to know if any of this excitation energy appears as kinetic energy of the fragments. This problem has been examined in two ways. First, we have prepared the compound nucleus Fm^{254} at an excitation energy of 117 MeV from bombardment of U^{238} with 166-MeV O^{16} ions. The value obtained for $\bar{E}_K$ for Fm^{254} prepared in this way is 185.6±4.0 MeV, compared with the value of 189.0±2.0 MeV determined by Brandt.[21]

This result was more thoroughly investigated in a second manner. The target Bi^{209} was bombarded with O^{16} ions at several excitation energies between 63 and 124 MeV. The data were treated as discussed previously; the resulting values for $\bar{E}_K$ as a function of excitation energy are shown in Fig. 9. Within the limits of error of these two checks, the average kinetic energy release is observed to be essentially independent of excitation energy. This agrees with previous results.[31,32]

If, as suggested by Halpern,[27] the energy of the fissioning system on descent from the saddle point is converted primarily into excitation energy of the final fragments, then $\overline{E}_K$ will depend almost entirely upon the Coulomb interaction between the fragments at scission, with little contribution from distortion motion. Thus, the kinetic energy release would be expected to be independent of the excitation energy, as observed. This argument lends support to a choice of scission shapes similar to the spheroid model with separation distance D = 0.2 (discussed in the previous section). Also, this argument implies that for a given fissioning nucleus, the distance between the fragments is constant, and, although it is not implicit in the argument, suggests a constant shape at scission.

C. Kinetic Energy Spread

In Fig. 10 we have plotted the measured full-width at the half-maximum value for the kinetic energy distribution as a function of x for both C^{12} and O^{16} bombardments. The excitation energies of the series of compound nuclei formed from each projectile vary over about a 20-MeV range. The plotted values for the half-widths were determined in the same manner as were the most probable kinetic energies. Although the limits of error are rather large, the data indicate a change in the kinetic energy spread of the fragments just above x = 0.7. Below this value the kinetic energy spread of the fragments is relatively constant while above it, a sharp increase in the distribution occurs.

These results can be readily explained in terms of the transition in equilibrium saddle shapes from the Frankel-Metropolis family to the Bohr-Wheeler family near x = 0.7, as discussed by Cohen and Swiatecki.[7] For x less than 0.7 the saddle shape and scission shape are nearly indentical; i.e.,

the saddle shape is nearly a two-fragment configuration. The length of time between the instant the nucleus passes over the saddle and the actual scission point is very short, thus preventing a wide spread in the properties of the fragments. The result is that the mass and kinetic energy distributions of the final fragments are to a large extent fixed by the saddle shape.

In contrast, as x increases above 0.7, the saddle shape becomes cylindrical in shape (Bohr-Wheeler family), thus differing substantially from the scission shape. During the time in which the nucleus is deforming from the saddle to the scission point, the nucleus is afforded the opportunity to divide along many paths. Therefore, a broadening of the properties of the final fragments would be expected.

The influence of the excitation energy on the half-width can be deduced from comparison of the curve for C^{12} bombardments with that from O^{16} bombardments. For the x values below 0.7, it is observed that the O^{16}-induced fission reactions lead to an increase in half width of about 6 MeV. About 20-25 MeV more excitation energy is brought in with 166-MeV O^{16} ions than with 125-MeV C^{12} ions. The rapidly changing slope of the curve makes such comparisons difficult for higher x values.

The effect of the excitation energy on the half-width for the $Bi^{209} + O^{16}$ system is shown in Fig. 11. A least-squares fit to this data shows that the half-width increases 0.13 MeV/MeV of excitation energy. These observations can be semiquantitatively explained by liquid-drop calculations.

Nix has shown that a zero-point vibrational energy of 1 MeV at the saddle point gives an intrinsic spread of about 11 to 12 MeV to the fragment kinetic energy distribution.[28] The large effect created by such a small amount of vibrational energy arises because of the strong dependence of the

Coulomb energy on the separation distance between the fragments. One can then explain the increase in half-width in terms of increased vibrational effects within the nucleus as the excitation energy increases

Qualitatively, the increase in half-width with increasing excitation energy is also in good agreement with the calculations of Nix. In order to obtain a quantitative comparison, it would be necessary to obtain the widths from a two-dimensional analysis of the fragment kinetic energies, rather than from single-fragment spectra. In addition, one should restrict himself to x values below 0.67.

IV. SUMMARY

Our results further substantiate that the primary factor responsible for the kinetic energy of fission fragments is mutual electrostatic repulsion. However, it is not possible to account for the data with a simple model based on the assumption of tangent spheres for the fragments at the scission point. Compared with the liquid-drop calculations of Cohen and Swiatecki,[26] the observed kinetic-energy-release data are quite consistent with scission shapes corresponding to either tangent spheroids or spheroids separated by a small distance. These scission shapes are similar to the Frankel-Metropolis family of saddle point shapes below x = 0.7. We have also confirmed the result that $\overline{E}_K$ is very nearly independent of excitation energy.

In agreement with the predications of Cohen and Swiatecki, we observe the fragment kinetic energy distribution to be nearly constant below x = 0.7. Above this value of x the kinetic energy distribution broadens quite rapidly. This behavior is related to the transition from the Frankel-Metropolis family of saddle shapes to the Bohr-Wheeler family near x = 0.7. The half-width is observed to increase with increasing excitation energy also, and can be explained in terms of the available energy for vibrational effects.

ACKNOWLEDGMENTS

The authors are especially indebted to Dr. W. J. Swiatecki for many hours of discussion concerning these experiments, and for making available to us his most recent calculations. His assistance was invaluable in the theoretical treatment of the data. We are also grateful to Dr. J. C. D. Milton and Ray Nix for use of the results of their theoretical calculations prior to publication. We wish to acknowledge Dr. Albert Ghiorso's interest in this work. We thank Daniel O'Connell and Gordon Steers for preparation of the excellent rare-earth targets. The solid-state detectors were provided by Robert M. Latimer and Walter E. Stockton. We thank William Goldsworthy for his assistance with the electronics and Mrs. Roberta Garrett for processing much of the data. The help of the HILAC crew in carrying out these experiments is also acknowledged.

FOOTNOTE AND REFERENCES

*Work done under the auspices of the U. S. Atomic Energy Commission.

1. N. Bohr and J. A. Wheeler, Phys. Rev. 56, 426 (1939).

2. J. Frankel, Phys. Rev. 55, 987 (1939).

3. J. Terrell, Phys.Rev. 113, 527 (1959).

4. W. J. Swiatecki, Phys.Rev. 101, 651 (1956).

5. W. J. Swiatecki, Phys. Rev. 104,993 (1956).

6. W. J. Swiatecki, Paper No. P/651, in Proceedings of the Second United Nations International Conference on the Peaceful Uses of Atomic Energy, (United Nations, Geneva, 1958), Vol. 15.

7. S. Cohen and W. J. Swiatecki, Ann. Phys. 19, 67 (1962).

8. T. Sikkeland, E. L. Haines, and V. E. Viola, Jr., Phys. Rev. 125, 1350 (1962).

9. J. Gilmore, S. G. Thompson, and I. Perlman, Phys. Rev. (in press).

10. We use the definitions of equilibrium saddle shapes given by Cohen and Swiatecki in reference 7. The Frankel-Metropolis family is the configuration which begins as two spheres in contact at x = 0, and as x increases, remains in the approximate shape of two fragments connected by a neck—i.e., a dumbbell-like shape. The Bohr-Wheeler family begins as a single sphere at x = 1 and deforms in a spheroidal fashion as x increases, giving a cylindrical shape. These two families intersect near x = 0.7. Recent work by Cohen and Swiatecki indicates that the distinction between the two families is not clear-cut, the transition from one family to the other being rapid, but not discontinuous.

11. R. M. Latimer (Lawrence Radiation Laboratory, Berkeley), private communication.

12. T. Sikkeland and V. E. Viola, Jr., (Lawrence Radiation Laboratory, Berkeley), unpublished data.

13. J. S. Fraser and J. C. Milton, Paper No. P/199, in Proceedings of the Second United Nations International Conference on the Peaceful Uses of Atomic Energy, (United Nations, Geneva, 1958), Vol. 15.

14. J. R. Alexander and M. F. Gadzik, Phys. Rev. 120, 874 (1960).

15. J. R. Huizenga and R. Vandenbosch, in Nuclear Reactions (North-Holland Publishing Co., Amsterdam, Netherlands, to be published), Vol. 2.

16. A. G. W. Cameron, Can. J. Phys. 35, 1021 (1957).

17. J. R. Huizenga, R. Chaudhry, and R. Vandenbosch, Phys. Rev. 126, 210 (1960).

18. T. Sikkeland and V. E. Viola, Jr., (Lawrence Radiation Laboratory, Berkeley), unpublished data from bombardments of several rare-earth targets between Pr^{141} and Lu^{175} with C^{12}, O^{16}, and Ne^{22} ions.

19. H. C. Britt and A. R. Quinton, Phys. Rev. 124, 877 (1961).

20. H. C. Britt, H. E. Wegner, and J. Gursky, Phys. Rev. Letters 8, 98 (1962); and H. C. Britt (Los Alamos Scientific Laboratory), private communication.

21. R. Brandt (Lawrence Radiation Laboratory, Berkeley), private communication. Recent spontaneous-fission values for other nuclei give E^{253}, 188± 3 MeV; Cf^{254}, 184± 3 MeV; Cf^{250}, 185± 3 MeV, and Cm^{248}, 179± 3 Mev. These latter values fall on our curve for $\bar{E}_K$ within the quoted limits of error.

22. R. Vandenbosch and J. R. Huizenga, Phys. Rev. 127, 212 (1962).

23. Swiatecki has pointed out that from the liquid-drop theoretical point of view, the data should be more appropriately correlated with a function

in which ξ depends and x rather than $\bar{E}_K$ with $Z^2/A^{1/3}$ as has been done previously. A least-squares best fit to the data for ξ as a general linear function of x gives

$$\xi = 0.243x + 0.0725.$$

From the definition of ξ and x, we may write

$$\bar{E}_K = 0.0863Z^2/A^{1/3} + 0.0725\,A^{2/3}.$$

Analysis of the data in this light also gives an excellent fit to the data.

24. A. E. S. Green, Revs. Modern Phys. 30, 569 (1958).

25. B. Hahn, D. G. Ravenhall, and R. Hofstadter, Phys Rev. 101, 1131 (1956).

26. S. Cohen and W. J. Swiatecki, The Deformation Energy of a Charged Drop: Part V: Results of Electronic Computer Studies, Lawrence Radiation Laboratory Report UCRL-10450, Aug. 30, 1962 (unpublished).

27. I. Halpern, Ann. Rev. Nuclear Sci. 9, 245 (1959).

28. J. R. Nix (Lawrence Radiation Laboratory, Berkeley), private communication.

29. J. C. D. Milton, Chalk River Scientific Laboratory, Ontatio, Canada, and B. M. Wilber, Lawrence Radiation Laboratory, Berkeley, unpublished results.

30. J. C. D. Milton and J. S. Fraser, Can. J. Pnys. (submitted for publication).

31. G. E. Gordon, A. E. Larsh, T. Sikkeland, and G. T. Seaborg, Phys. Rev. 120, 1341 (1960).

32. H. C. Britt and A. R. Quinton, Phys. Rev. 120, 1768 (1960).

Table I. Properties of various fissioning species for which $\bar{E}_K$ has been measured in this work.[a]

Heavy Ion	Target	Compound Nucleus	$Z^2/A^{1/3}$	$\bar{E}_{c.m.}^{f}$	$\bar{\nu}$	$\bar{E}_{c.m.}^{i}$	x_{CN}	Exp. ξ
	Tb^{159}	Lu^{171}	908.2	113.2	6	117.5±4.8	0.588	0.214±0.009
	Ho^{165}	Ta^{177}	979.1	117.2	7	122.0±5.2	0.598	0.217±0.010
	Tm^{169}	Re^{181}	994.4	116.6	8	122.3±4.2	0.616	0.215±0.007
	Lu^{175}	Ir^{187}	1037	125.8	8	131.4±3.6	0.630	0.226±0.006
125-MeV C^{12}	Au^{197}	At^{209}	1217	140.6	8	147.2±3.6	0.688	0.235±0.005
	Bi^{209}	Ac^{221}	1310	152.0	9	158.7±3.0	0.712	0.244±0.004
	Th^{232}	Cm^{244}	1475	167.6	12	176.3±8.8	0.751	0.253±0.013
	U^{238}	Cf^{250}	1525	174.4	12	183.2±4.0	0.763	0.259±0.006
	Pu^{240}	Fm^{252}	1583	176.0	13	185.6±4.6	0.789	0.261±0.006
	Pr^{141}	Ho^{157}	832.1	106.2	7	111.2±6.6	0.569	0.215±0.013
	Tb^{159}	Ta^{175}	952.7	118.6	8	124.3±4.4	0.606	0.223±0.008
	Ho^{165}	Re^{181}	994.4	121.0	9	127.3±5.4	0.618	0.223±0.010
	Tm^{169}	Ir^{185}	1041	125.8	9	132.2±4.0	0.636	0.229±0.006
166-MeV O^{16}	Lu^{175}	Au^{191}	1084	130.6	10	137.8±3.8	0.650	0.223±0.006
	Au^{197}	Fr^{213}	1267	147.6	11	155.6±3.4	0.706	0.245±0.005
	Bi^{209}	Pa^{225}	1362	158.2	11	166.3±3.0	0.732	0.252±0.005
	Th^{232}	Cf^{248}	1529	179.4	14	190.1±8.8	0.772	0.268±0.012
	U^{238}	Fm^{254}	1579	174.6	15	185.6±4.0	0.783	0.260±0.005
	Pu^{240}	102^{256}	1641	181.4	15	192.7±4.6	0.807	0.268±0.007

[a] The values are based on $\bar{E}_{c.m.}^{f}$ = 103 MeV for the Cf^{252} light peak (from the value of $\bar{E}_{c.m.}^{i}$ = 104.7 MeV of reference 13).

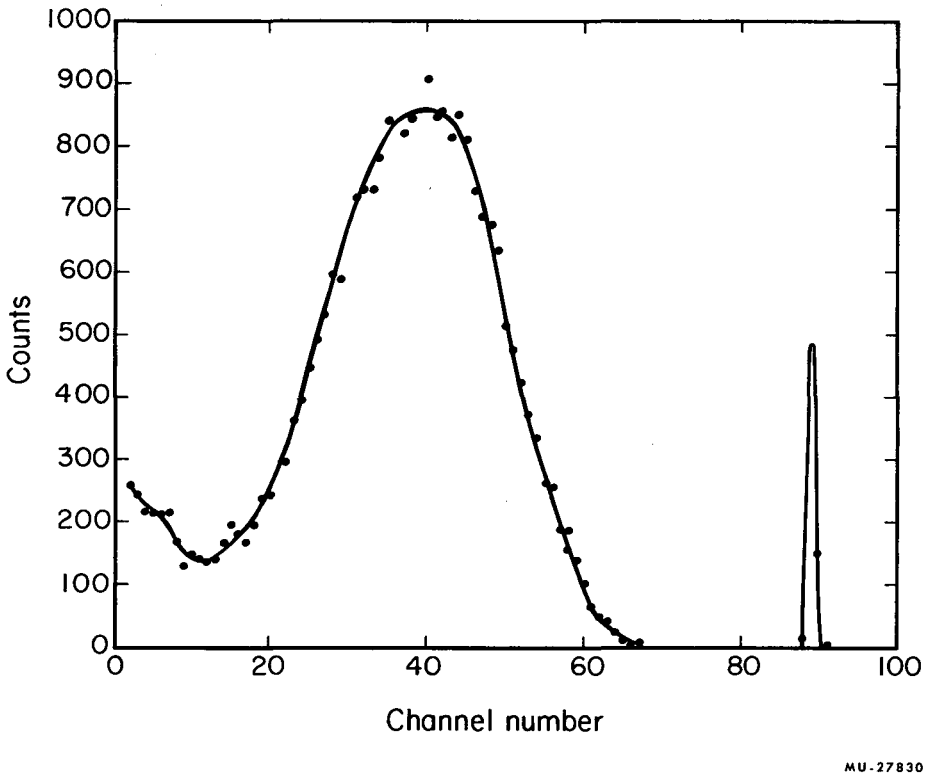

Fig. 1. Pulse-height spectrum from Bi^{209} bombarded with 166-MeV O^{16} ions.

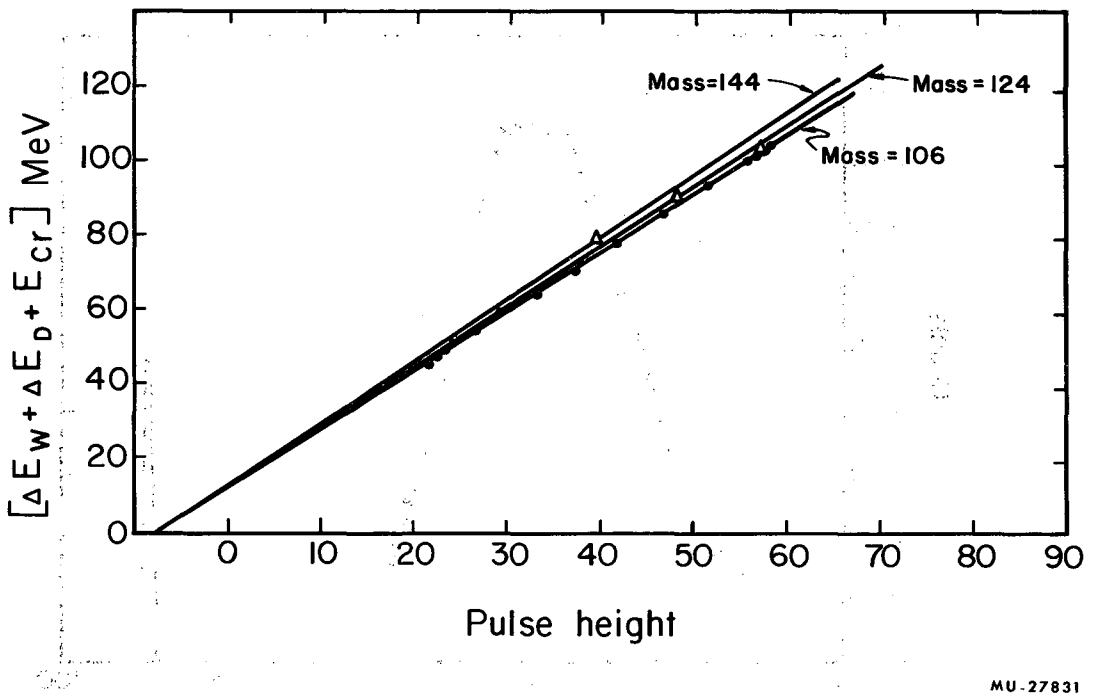

Fig. 2. Pulse height vs energy calibration curve. Circles (●) represent results from bombardment of Bi^{209} with 166-MeV O^{16} ions at various angles; triangles represent Cf^{252} energies discussed in the text.

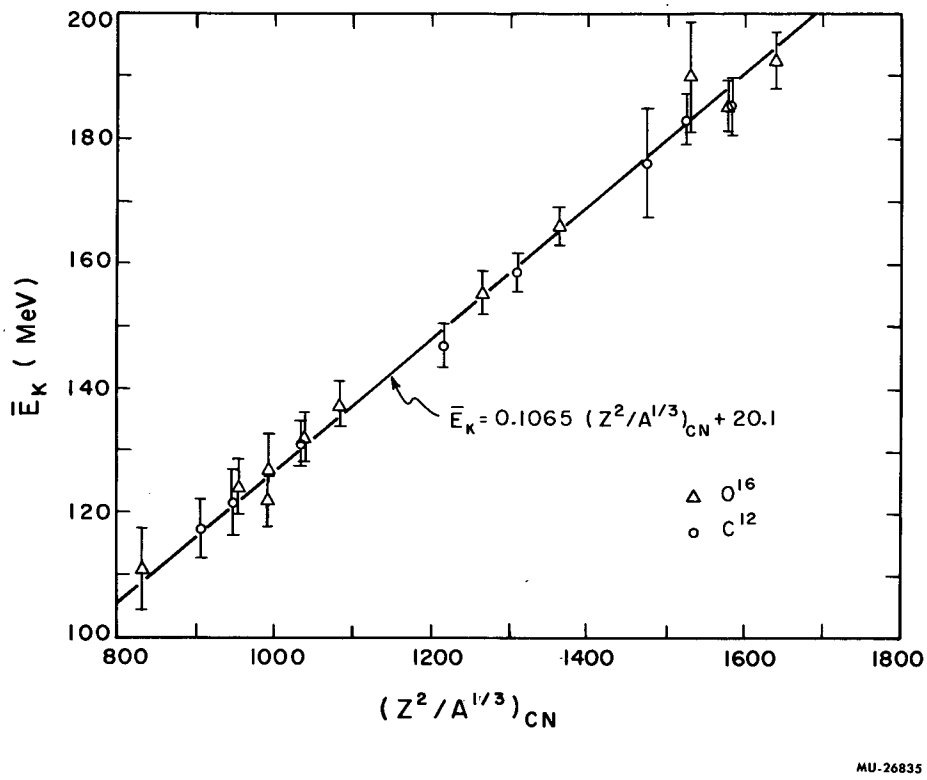

Fig. 3. Plot of $\bar{E}_K$ versus $Z^2/A^{1/3}$ for the fissioning nuclei studied in this work.

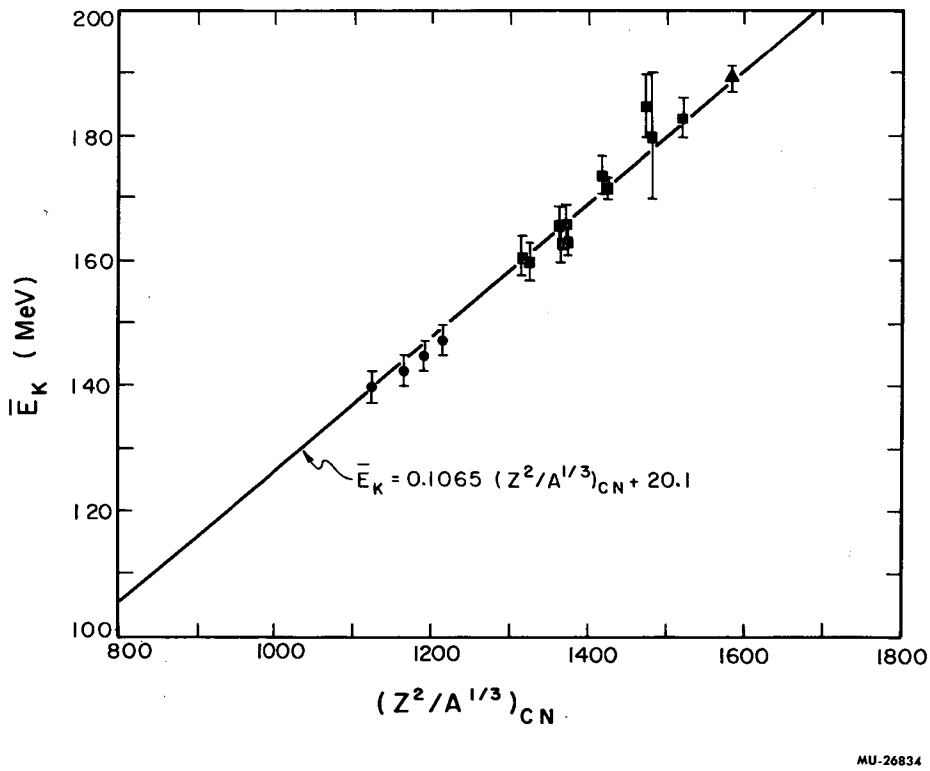

Fig. 4. Plot of $\bar{E}_K$ versus $Z^2/A^{1/3}$ for data obtained elsewhere. Squares (■) represent results from reference 3; circles (●) are from reference 20, and the triangle (▲) is from reference 21.

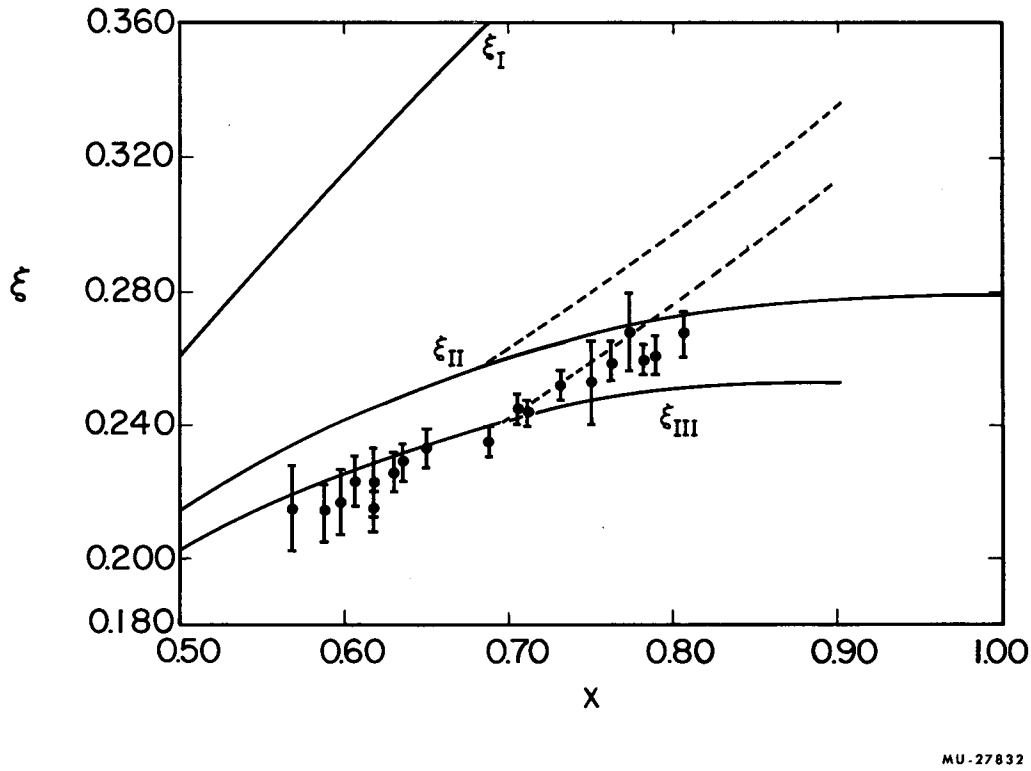

Fig. 5. Experimental values of the electrostatic interaction energy as a function of the fissionability parameter x. Solid and dashed lines are calculated results for ξ_I, ξ_{II} and ξ_{III} (discussed in Sec. III-A of the text).

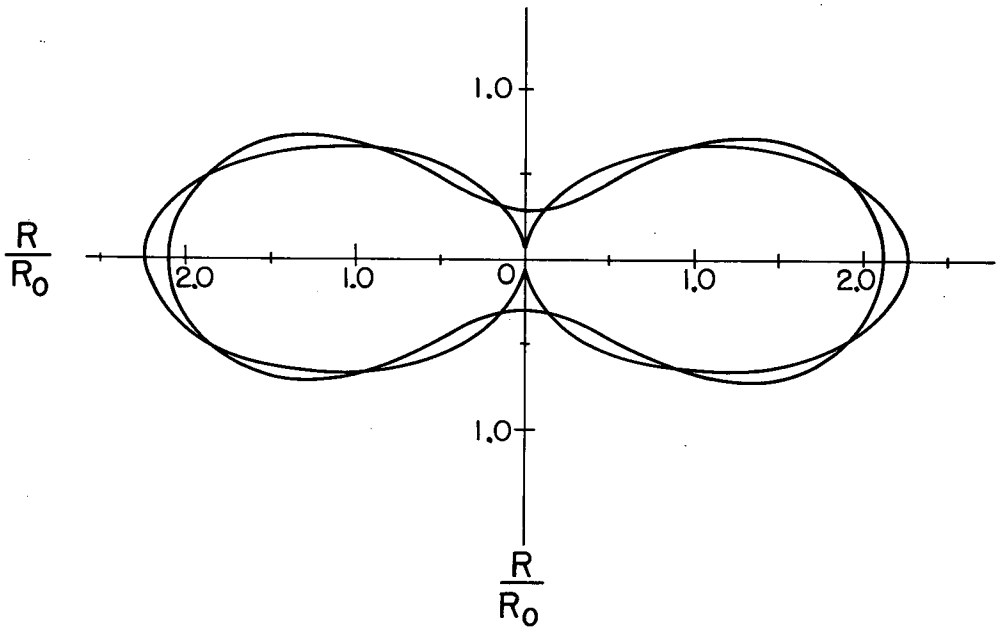

Fig. 6. Comparison of the equilibrium saddle shape from the Legendre polynomial expansion for x = 0.60 with the configuration of tangent spheroids with a ratio of axes C/A = 1.674, the optimum ratio for x = 0.60.

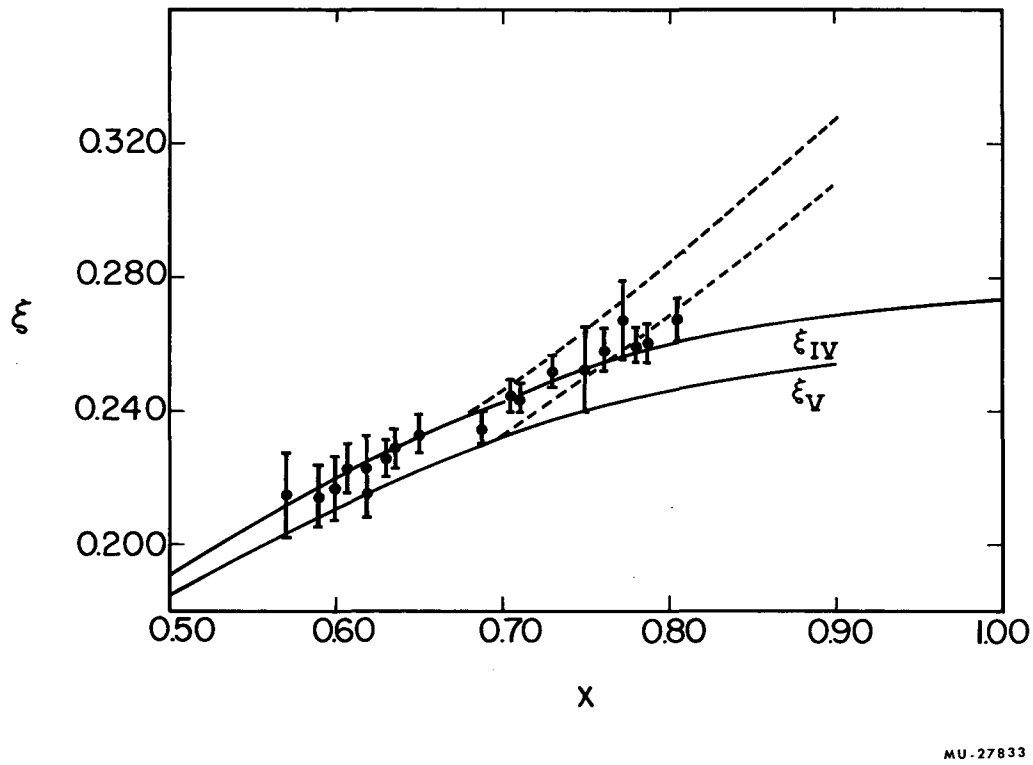

Fig. 7. Experimental values of the electrostatic interaction energy as a function of the fissionability parameter x. Solid and dashed lines are calculated results for ξ_{IV} and ξ_V (discussed in text).

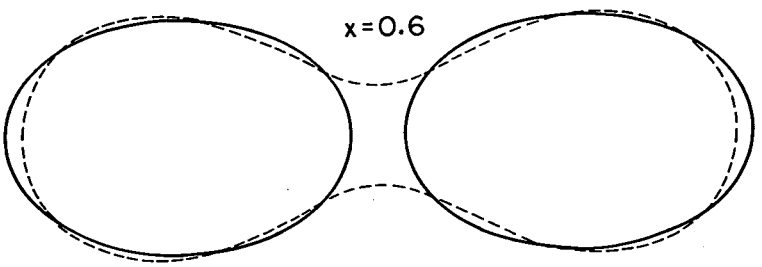

MU-27997

Fig. 8. Comparison of the equilibrium saddle shape from the Legendre polynomial expansion for x = 0.60 with the configuration of spheroids separated by a distance D = 0.2 with a ratio of C/A 1.474, the optimum ratio for x = 0.60.

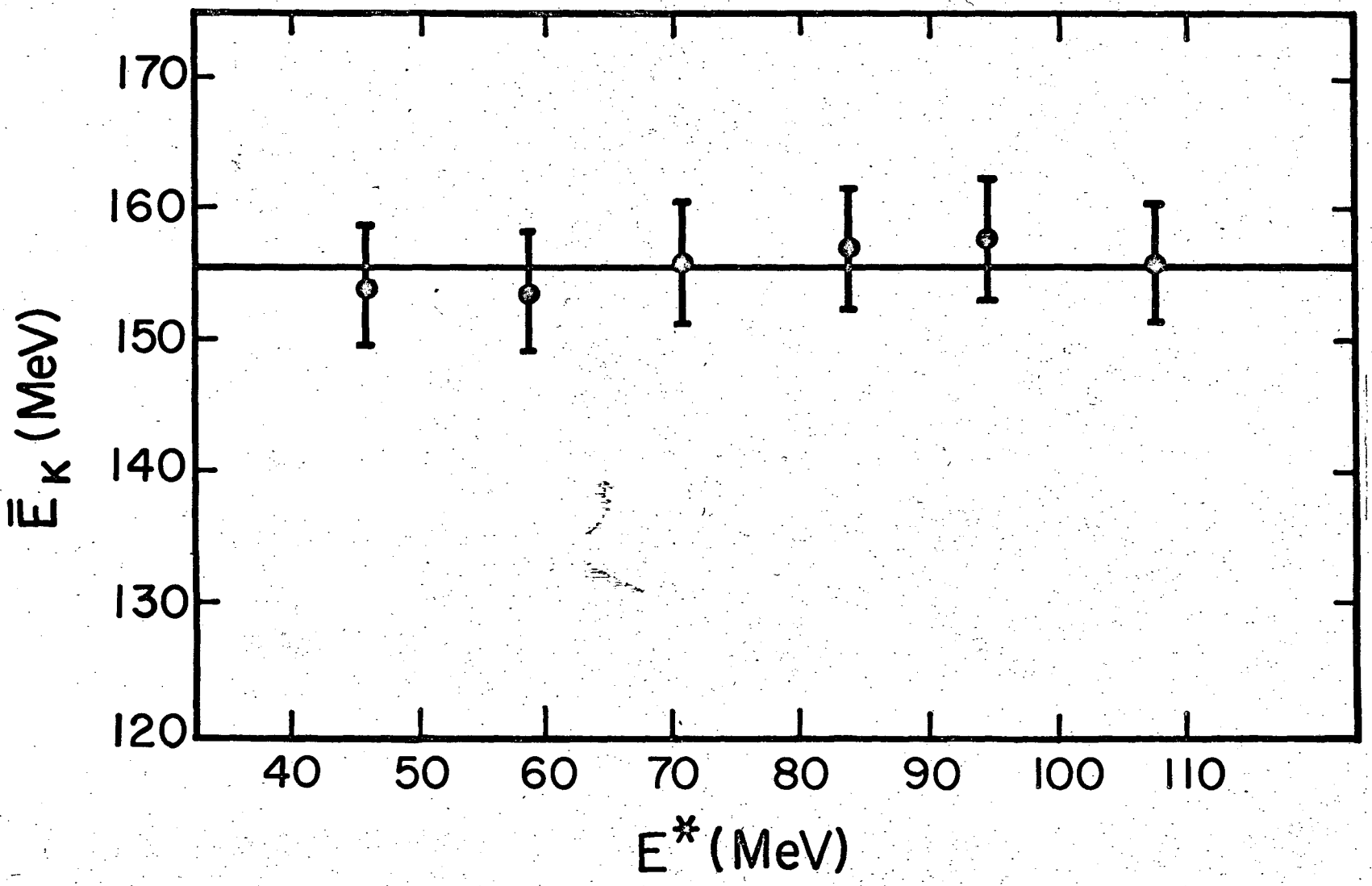

Fig. 9. Average kinetic energy release as a function of the excitation energy of the compound nucleus formed from bombardment of Bi^{209} with O^{16} ions.

MU-27835

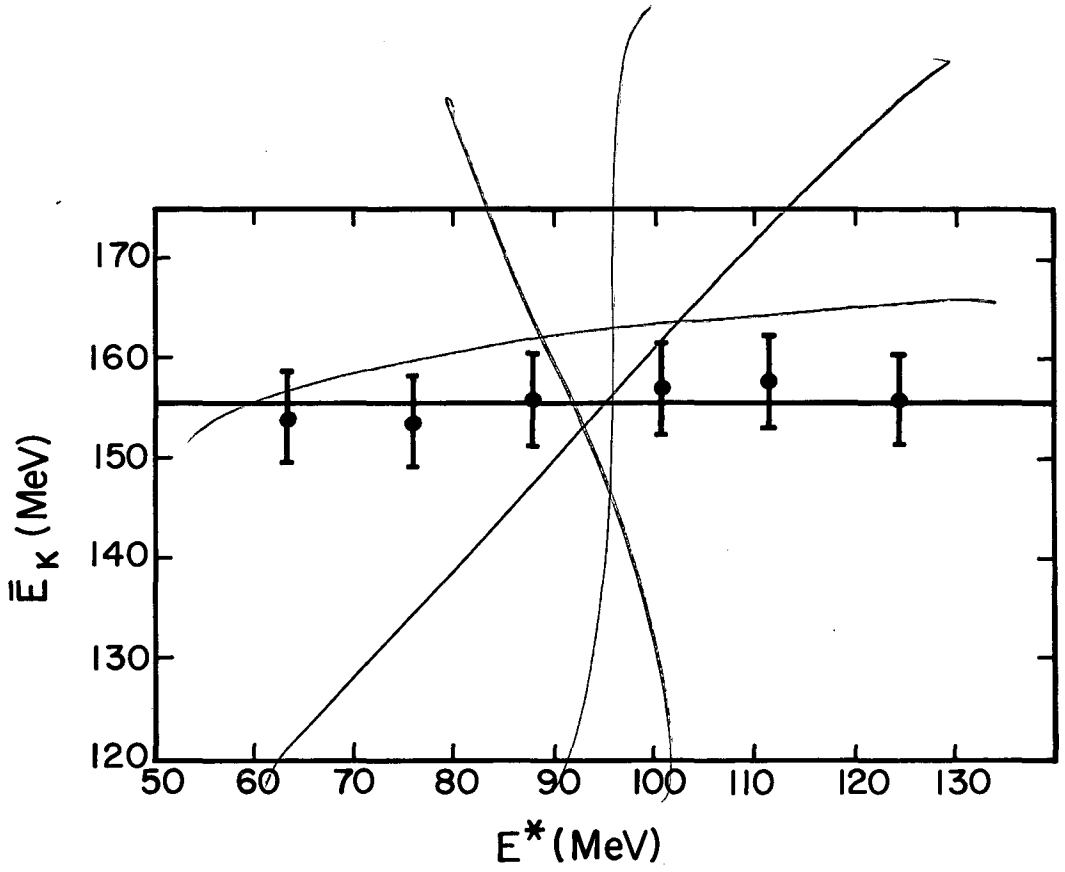

Fig. 9. Average kinetic energy release as a function of the excitation energy of the compound nucleus formed from bombardment of Bi^{209} with O^{16} ions.

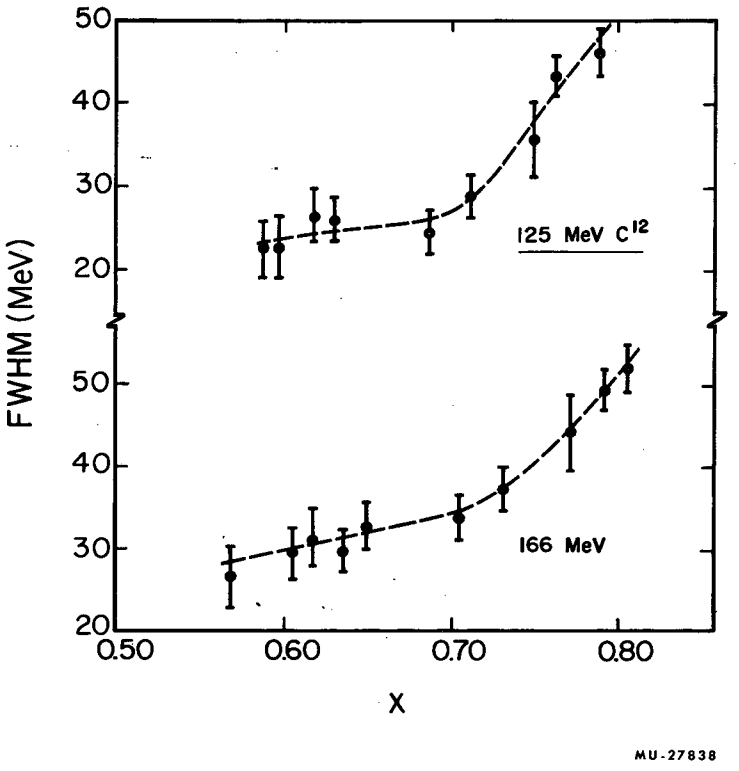

Fig. 10. Full-width at half maximum of the fission fragment kinetic energy spectrum as a function of x of the fissioning nucleus for C^{12} bombardments (upper curve) and O^{16} bombardments (lower curve).

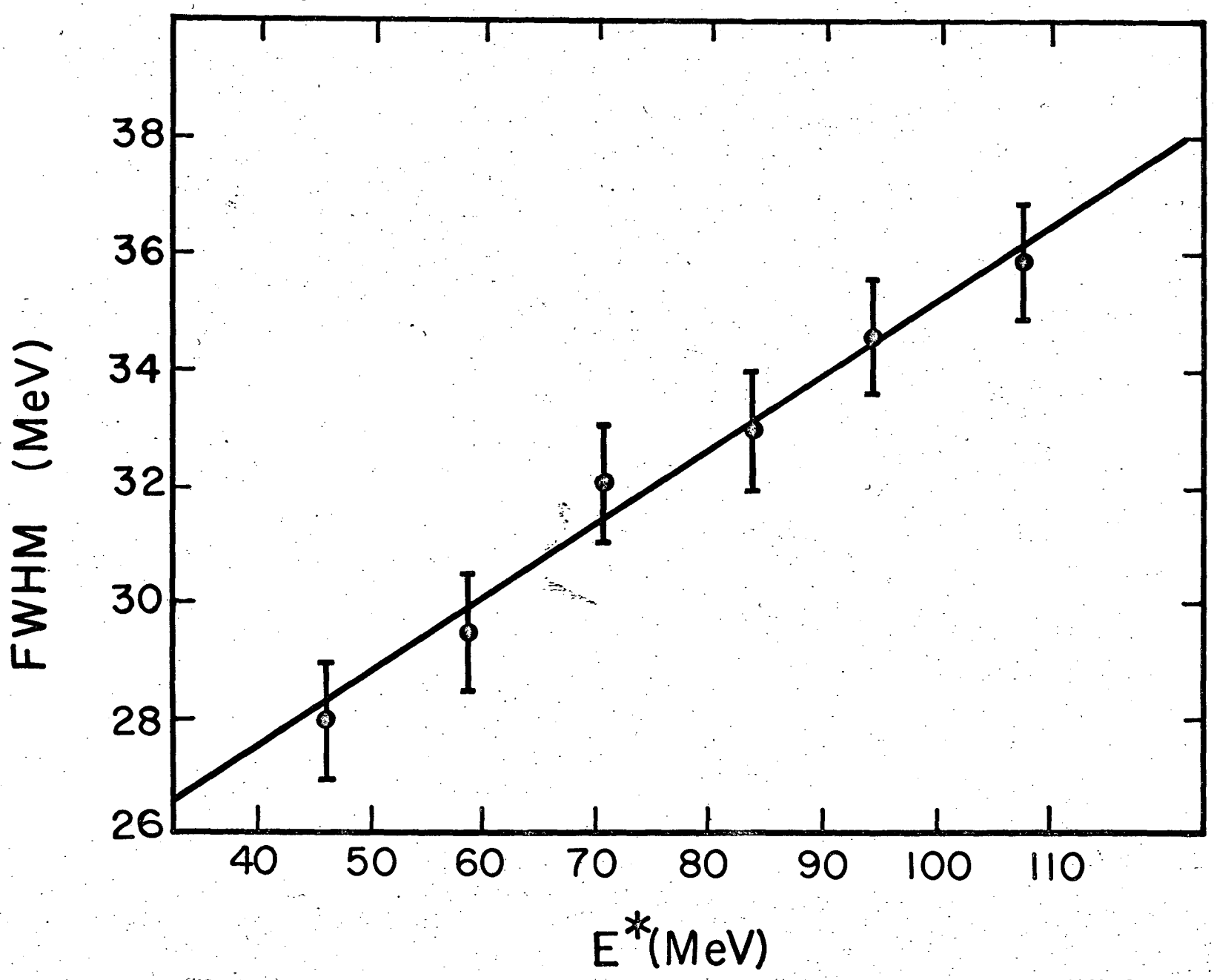

MU-27836

Fig. 11. Full-width at half maximum of the fission fragment kinetic energy spectrum for bombardment of Bi^{209} with O^{16} ions at several excitation energies.

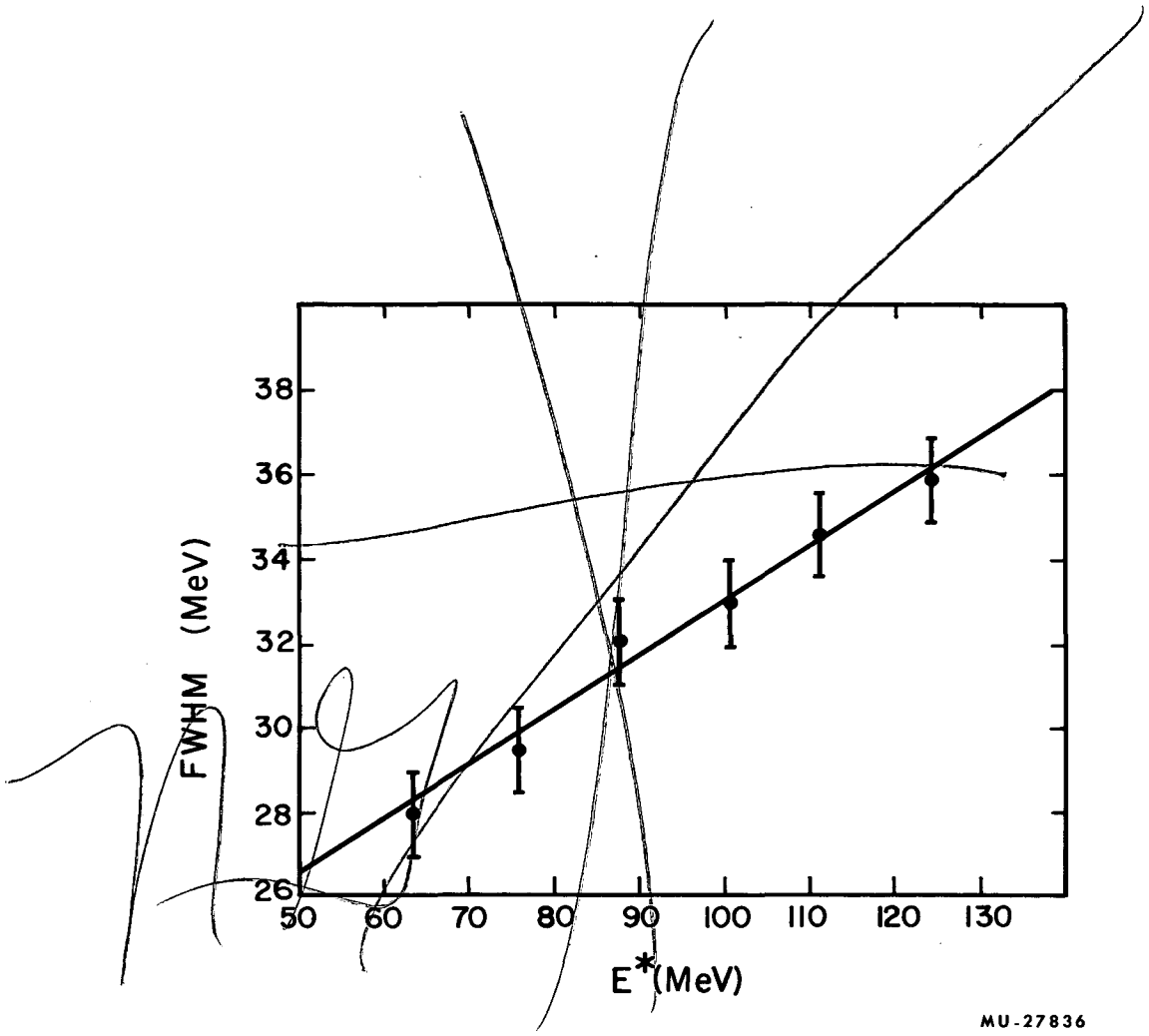

Fig. 11. Full-width at half maximum of the fission fragment kinetic energy spectrum for bombardment of Bi^{209} with O^{16} ions at several excitation energies.